

# Time Change and Universality in Turbulence and Finance

Ole E. Barndorff-Nielsen, Jürgen Schmiegel  
*Thiele Centre for Applied Mathematics in Natural Science,  
Department of Mathematical Sciences, University of Aarhus, Denmark*  
and Neil Shephard  
*Department of Economics, University of Oxford, UK*

October 16, 2006

## Abstract

Empirical time series of turbulent flows and financial markets reveal some common basic stylized features. In particular, the densities of velocity increments and log returns are well fitted within the class of Normal inverse Gaussian distributions and show a similar evolution across time scales with the heaviness of the tails decreasing with increasing time scale. We report empirical findings about the universality of the evolution of the densities of velocity increments/log returns across time scales. In terms of an intrinsic deterministic time change, the densities of velocity increments for various turbulent flows behave in a universal fashion. The same type of universality is found in financial markets.

Keywords: FX-markets; normal inverse Gaussian; stochastic equivalence; time change; turbulence; universality.

## 1 Introduction

The statistics of turbulent flows and financial markets share a number of stylized features (Ghashgaie et al (1996), Peinke et al (2004) and Barndorff-Nielsen (1998a)). The counterpart of the velocity in turbulence are log prices in finance and velocity increments play the role of log returns. The equivalent of the intermittency of the energy dissipation in turbulence is the strong variability of the volatility in financial markets. The most important similarities between both fields are semiheavy tails for the distributions of log returns/velocity increments, the evolution of the densities of log returns/velocity increments across time scales with the heaviness of the tails decreasing as the time scale increases and long range dependence of absolute log returns/velocity increments. It is important to note that long range dependencies are only observed for the absolute price process while the velocity field itself shows algebraic decay of the autocorrelation function. Other important differences are the skewness of the densities of velocity increments in contrast to the symmetry of the distribution of log returns in FX markets and the different behaviour of bipower variation (Barndorff-Nielsen and Shephard (2004)) due to the particular small time scale behaviour of the velocity autocorrelation function (Barndorff-Nielsen et al (2006)).

Intermittency/volatility is related to the heaviness of the tails and the non-Gaussianity of the distribution of velocity increments and log returns. In this respect, Normal inverse Gaussian (NIG) distributions are a suitable class of probability distributions which fit the

empirical densities in both systems to high accuracy (Barndorff-Nielsen (1995,1997), Rydberg (1997), Forsberg (2002), Barndorff-Nielsen et al (2004) and Barndorff-Nielsen and Schmiegel (2006)). Moreover, it has been shown in Barndorff-Nielsen et al (2004) and Barndorff-Nielsen and Schmiegel (2006) that the analysis of velocity increments within the NIG class reveals some hidden type of universality which relates the statistical properties of widely different turbulent flows by a simple deterministic time change. In view of the similarities between turbulence and finance, it is natural to ask about the existence of an intrinsic deterministic time change in finance which relates the densities of log returns for different markets in an universal way.

In this paper we investigate the existence of a stochastic equivalence class (SEC) for log returns in financial markets. It turns out that the variance of log returns acts as an internal clock in terms of which the densities of log returns from different markets collapse. We support the existence of such a stochastic equivalence class by empirically studying the behaviour of various currency returns and some metal returns.

In Section 2 we provide some background material on NIG distributions which are central for the description of the densities of velocity increments and log returns. The notion of SEC in turbulence is briefly outlined in Section 3. Section 4 discusses the corresponding results for financial markets. Section 5 concludes.

## 2 Normal inverse Gaussian law

The normal inverse Gaussian law, with parameters  $\alpha, \beta, \mu$  and  $\delta$ , is the distribution on the real axis  $\mathbf{R}$  having probability density function

$$p(x; \alpha, \beta, \mu, \delta) = a(\alpha, \beta, \mu, \delta) q \left( \frac{x - \mu}{\delta} \right) q \left( \frac{x - \mu}{\delta} \right)^{-1} K_1 \left\{ \delta \alpha q \left( \frac{x - \mu}{\delta} \right) \right\} e^{\beta x} \quad (1)$$

where  $q(x) = \sqrt{1 + x^2}$  and

$$a(\alpha, \beta, \mu, \delta) = \pi^{-1} \alpha \exp \left\{ \delta \sqrt{\alpha^2 - \beta^2} - \beta \mu \right\} \quad (2)$$

and where  $K_1$  is the modified Bessel function of the third kind and index 1. The domain of variation of the parameters is given by  $\mu \in \mathbf{R}$ ,  $\delta \in \mathbf{R}_+$ , and  $0 \leq |\beta| < \alpha$ . The distribution is denoted by  $\text{NIG}(\alpha, \beta, \mu, \delta)$ .

If  $X$  is a random variable with distribution  $\text{NIG}(\alpha, \beta, \mu, \delta)$  then the cumulant generating function of  $X$ , i.e.  $K(\theta; \alpha, \beta, \mu, \delta) = \log E\{e^{\theta X}\}$ , has the form

$$K(\theta; \alpha, \beta, \mu, \delta) = \delta \left\{ \sqrt{\alpha^2 - \beta^2} - \sqrt{\alpha^2 - (\beta + \theta)^2} \right\} + \mu \theta. \quad (3)$$

It follows immediately from this that if  $x_1, \dots, x_m$  are independent normal inverse Gaussian random variables with common parameters  $\alpha$  and  $\beta$  but individual location-scale parameters  $\mu_i$  and  $\delta_i$  ( $i = 1, \dots, m$ ) then  $x_+ = x_1 + \dots + x_m$  is again distributed according to a normal inverse Gaussian law, with parameters  $(\alpha, \beta, \mu_+, \delta_+)$ .

Furthermore, the first four cumulants of  $\text{NIG}(\alpha, \beta, \mu, \delta)$ , obtained by differentiation of (3), are found to be

$$\kappa_1 = \mu + \frac{\delta \rho}{\sqrt{1 - \rho^2}}, \quad \kappa_2 = \frac{\delta}{\alpha(1 - \rho^2)^{3/2}} \quad (4)$$

and

$$\kappa_3 = \frac{3\delta\rho}{\alpha^2(1-\rho^2)^{5/2}}, \quad \kappa_4 = \frac{3\delta(1+4\rho^2)}{\alpha^3(1-\rho^2)^{7/2}}, \quad (5)$$

where  $\rho = \beta/\alpha$ . Hence, the standardised third and fourth cumulants are

$$\begin{aligned} \bar{\kappa}_3 &= \frac{\kappa_3}{\kappa_2^{3/2}} = 3 \frac{\rho}{\{\delta\alpha(1-\rho^2)^{1/2}\}^{1/2}} \\ \bar{\kappa}_4 &= \frac{\kappa_4}{\kappa_2^2} = 3 \frac{1+4\rho^2}{\delta\alpha(1-\rho^2)^{1/2}}. \end{aligned} \quad (6)$$

We note that the NIG distribution (1) has semiheavy tails; specifically,

$$p(x; \alpha, \beta, \mu, \delta) \sim \text{const. } |x|^{-3/2} \exp(-\alpha|x| + \beta x), \quad x \rightarrow \pm\infty \quad (7)$$

as follows from the asymptotic relation

$$K_\nu(x) \sim \sqrt{2/\pi x}^{-1/2} e^{-x} \quad \text{as } x \rightarrow \infty. \quad (8)$$

The normal inverse Gaussian law  $\text{NIG}(\alpha, \beta, \mu, \delta)$  has the following important characterisation in terms of the bivariate Brownian motion with drift. Let  $B(t) = \{B_1(t), B_2(t)\}$  be a bivariate Brownian motion starting at  $(\mu, 0)$  and having drift vector  $(\beta, \gamma)$  where  $\beta \in \mathbf{R}$  and  $\gamma \geq 0$ . Furthermore, let  $T$  denote the time when  $B_1$  first reaches level  $\delta > 0$  and let  $X = B_2(T)$ . Then  $X \sim \text{NIG}(\alpha, \beta, \mu, \delta)$  with  $\alpha = \sqrt{\beta^2 + \gamma^2}$ .

It is often of interest to consider alternative parametrisations of the normal inverse Gaussian laws. In particular, letting  $\bar{\alpha} = \delta\alpha$  and  $\bar{\beta} = \delta\beta$ , we have that  $\bar{\alpha}$  and  $\bar{\beta}$  are invariant under location—scale changes.

**NIG shape triangle** For some purposes it is useful, instead of the classical skewness and kurtosis quantities (6), to work with the alternative asymmetry and steepness parameters  $\chi$  and  $\xi$  defined by

$$\chi = \rho\xi \quad (9)$$

and

$$\xi = (1 + \bar{\gamma})^{-1/2} \quad (10)$$

where  $\rho = \beta/\alpha = \bar{\beta}/\bar{\alpha}$  and  $\bar{\gamma} = \delta\gamma = \delta\sqrt{\alpha^2 - \beta^2}$ . Like  $\bar{\kappa}_3$  and  $\bar{\kappa}_4$ , these parameters are invariant under location-scale changes and the domain of variation for  $(\chi, \xi)$  is the *normal inverse Gaussian shape triangle*

$$\{(\chi, \xi) : -1 < \chi < 1, 0 < \xi < 1\}.$$

The distributions with  $\chi = 0$  are symmetric, and the normal and Cauchy laws occur as limiting cases for  $(\chi, \xi)$  near to  $(0, 0)$  and  $(0, 1)$ , respectively. Figure 1 gives an impression of the shape of the NIG distributions for various values of  $(\chi, \xi)$ .

A systematic study of the class of normal inverse Gaussian distributions, and of associated stochastic processes, was begun in Barndorff-Nielsen (1995,1997,1998a,1998b,1998c). Further theoretical developments and applications are discussed in Rydberg (1997,1999), Prause (1999), Eberlein (2000), Raible (2000), Barndorff-Nielsen and Shephard (2000,2001,2002,2007), Barndorff-Nielsen et al (2004), Barndorff-Nielsen and Schmiegel (2006), Barndorff-Nielsen and

Prause (2001), Barndorff-Nielsen and Levendorskiĭ (2001), Asmussen and Rosinski (2001), Cont and Tankov (2004), Forsberg (2002) and McNeil et al (2005). As discussed in the papers cited and in references given there, the class of NIG distributions and processes have been found to provide accurate modelling of a great variety of empirical findings in the physical sciences and in financial econometrics. (The wider class of generalised hyperbolic distributions, introduced in Barndorff-Nielsen (1977), provides additional possibilities for realistic modelling of dynamical processes, see references in the papers cited above.)

### 3 Time change and universality for turbulent flows

Typical turbulent data sets consist of one-point time records of the longitudinal (along the mean flow) velocity component and the quantity of interest are turbulent velocity increments

$$u_s = v(t + s) - v(t), \quad (11)$$

where  $v(t)$  denotes the longitudinal one-point velocity component at time  $t$ .

It has been shown in Barndorff-Nielsen et al (2004) and Barndorff-Nielsen and Schmiegel (2006) that the densities of velocity increments from different isotropic turbulent flow experiments with widely different flow conditions are well fitted within the class of NIG distributions and collapse after applying a deterministic intrinsic time change from  $s$  to  $\delta(s)$ , where  $\delta(s)$  denotes the scale parameter of the approximate NIG distributions at time scale  $s$ .

Obviously, any monotonically increasing function (the same for all data sets) of the scale parameter  $\delta(s)$  may equally well be used as an intrinsic time change. In particular, the variance  $c_2(s)$  of velocity increments at time scale  $s$  increase monotonically as a universal function of the scale parameter  $\delta(s)$ . The universal dependence of the variance  $c_2(s)$  on the scale parameter  $\delta(s)$  is a striking property in turbulence and can not be expected in general. In fact, for the financial data sets analyzed in Section 4, the variances depend on the scale parameter in a non-universal way and  $\delta(s)$  does not serve as an intrinsic time change. We therefore use the variance  $c_2(s)$  as the intrinsic time change for the comparison of turbulence with financial data.

Figure 2 shows, as an example, the approximation of the densities of velocity increments  $u_s$  within the class of NIG distributions for various time scales  $s$ . The data are from a helium jet experiment. We performed the same analysis for all time scales that allow for a proper estimation of the parameters of the approximate NIG distributions. The evolution of the densities of velocity increments for time scales  $s \in [4, 8000]$  (in units of the finest resolution of the data set) within the NIG shape triangle is shown in Figure 3. We clearly observe the evolution from heavy tails at small time scales towards a Gaussian shape at large time scales. In terms of the variances acting as an intrinsic time change, this evolution across time scales is universal. Figure 4 shows the collapse of the densities of velocity increments obtained from widely different isotropic flow experiments at time scales  $s$  where the variances  $c_2(s)$  are the same. After applying a time change from time scale  $s$  to the variance  $c_2(s)$  the densities of velocity increments from widely different data sets collapse onto universal distributions, independent of the flow conditions (Barndorff-Nielsen and Schmiegel (2006)). The data sets used are time series of the velocity  $v(t)$  from helium jet experiments (data sets (*h85*), (*h124*), (*h283*), (*h352*), (*h703*), (*h885*) and (*h929*)), from an atmospheric boundary layer experiment (data set (*at*)) and from a wind tunnel experiment (data set (*w*)). Each data set is normalized by its standard deviation. For more details about the data sets we refer to Chanal et al (2000)

for the helium jet experiments, to Dhruva (2000) and Sreenivasan and Dhruva (1998) for the atmospheric boundary layer experiment and to Antonia and Pearson (2000) for the wind tunnel experiment.

The collapse of the densities of velocity increments can be put into more mathematical terms by introducing a stochastic equivalence class of the form

$$u_{s_1}^{(i)} \stackrel{d}{=} u_{s_2}^{(j)} \Leftrightarrow c_2^{(i)}(s_1) = c_2^{(j)}(s_2) \quad (12)$$

where  $\stackrel{d}{=}$  denotes equality in distribution and the superscripts  $(i)$  and  $(j)$  label different experiments. Relation (12) states that the densities of velocity increments follow a one-parameter curve in the space of probability densities. Each individual data set covers a certain part of this one-parameter curve. It is the variance  $c_2(s)$  that accounts for the individual characteristics of each data set and determines the location onto this one-parameter curve.

## 4 Time change and universality in FX-markets

The appropriateness of NIG distributions for describing the densities of increments of both processes, turbulent velocities and log prices in financial markets, as well as other similarities between the turbulent and financial regimes may naturally pose the hypothesis of an intrinsic deterministic time change in financial markets leading to a similar collapse of the marginal densities of log returns as observed in turbulence. We would like to stress that this hypothesis, for the time being, only addresses the evolution of the marginal densities of increments across time scales. In Section 5 we briefly discuss the dynamic extension of the results discussed in the present paper.

### 4.1 The data sets

For the empirical verification of our hypothesis about the existence of a deterministic time change, resulting in a collapse of the marginal distributions of log returns, we analyze two different types of financial data sets. The first group of data comprises part of the Olsen & Associates data set HFDF96 and consists of 30 *min* log returns covering the year 1996. We analyze 11 FX markets (AUD/USD, DEM/FIM, DEM/ITL, GBP/USD, USD/CHF, USD/FIM, USD/FRF, USD/ITL, USD/NLG, USD/XEU, USD/ZAR) and 3 Metal markets (XAG/USD, XPD/USD, XPT/USD). The second group of data sets consists of 5 *min* DEM/USD and JPY/USD log returns with 705312 observations each. A detailed description of the data sets can be found in Dacorogna et al (2001).

### 4.2 The distribution of log returns

Figure 5 shows, as an example, the log densities of DEM/USD log returns at various time scales  $s$  and the corresponding approximation of these densities within the class of NIG distributions obtained from maximum likelihood estimation of the four NIG parameters  $\alpha$ ,  $\beta$ ,  $\delta$  and  $\mu$ . We observe the evolution of the densities of log returns with decreasing heaviness of the tails as the time scale  $s$  increases. This evolution across scales is analogous to what is observed for the densities of velocity increments in a turbulent flow (see Figure 2). We performed the same analysis for time scales  $s \in [1, 290]$  (in units of 5 *min*). Figure 6 shows the NIG shape triangle for DEM/USD log returns. As for turbulence (see Figure 3) we observe

the evolution towards the Gaussian limit. However, in contrast to the turbulence data sets, the densities of log returns are symmetric ( $\chi \approx 0$ ).

We compare the evolutions across time scales of log returns for all of our financial data sets in Figure 7 which shows the variances  $c_2(s)$  as a function of the time scale  $s$  in double logarithmic representation. Note that in general the variances  $c_2(s)$  are not linear in  $s$ , otherwise we would expect the plots of the variances of the various financial data sets to be parallel in the double logarithmic representation of Figure 7.

### 4.3 Collapse of densities

The empirical verification of the SEC relation (12) for financial markets requires that, whenever the variances  $c_2^{(i)}(s^{(i)})$  and  $c_2^{(j)}(s^{(j)})$  are equal, the corresponding densities of log returns at time scales  $s^{(i)}$  and  $s^{(j)}$  collapse. Here the superscripts  $(i)$  and  $(j)$  denote different financial markets. Denoting the inverse of  $c_2$  by  $\bar{c}_2$  we may directly relate the time scales  $s^{(i)}$  and  $s^{(j)}$

$$s^{(i)} = \bar{c}_2^{(i)}(c_2^{(j)}(s^{(j)})). \quad (13)$$

This relation establishes the intrinsic time change from market  $(j)$  to some other market  $(i)$ . Figure 8 shows the intrinsic time change between DEM/USD log returns and JPY/USD log returns obtained from Figure 7 by fixing certain values of the variances and reading off the time scales that correspond to these fixed variances. Note that the time change appears to be linear. Such a linearity holds if and only if the variances behave as  $c_2^{(i)}(as) = c_2^{(j)}(s)$  where  $a$  is a constant (depending on  $(i)$  and  $(j)$ ).

As an illustration we refer to Figures 11(a) and 11(i) which show that the corresponding densities of log DEM/USD returns and JPY/USD log returns indeed collapse when transforming the time scales according to Figure 8.

We performed the same analysis for all our financial data sets, i.e. we fixed a certain value of the variance in Figure 7 and read off the time scale for each market that corresponds to this fixed variance. In accordance with the SEC relation (12), the corresponding densities of log returns collapse for all our data sets. Figure 9 shows two examples for the collapse of the densities of currency log returns. For USD/CHF and DEM/FIM log returns the densities of equal time log returns are very different. Applying the time change (13) shows that the log returns of equal variance time scales collapse. In this example the corresponding equal variance time scales are 1  $h$  and 4  $h$  for the USD/CHF and DEM/FIM log returns, respectively.

For the second example in Figure 9 the difference between equal time densities is much smaller than for the previous example. But again, the equal variance densities collapse.

Figure 10 shows two examples for the collapse of the densities of currency log returns and metal log returns, again confirming the SEC relation (12). The deviations at very small and at very large log returns are negligible (compare to Figure 11(h)).

The analysis of our financial data sets confirms the existence of a SEC relation (12) for FX markets and Metal markets. We therefore claim that to a high degree of accuracy the marginal densities of log returns for these markets follow a one parameter curve in the space of probability densities. The characteristic parameter for the location of the marginal distributions of log returns for each data set onto this universal curve in the space of probability densities is the variance as a function of the time scale  $s$  which comprises the individual characteristics of the each market (concerning the evolution of the densities of log returns across time scales) but in terms of which the marginal distributions of log returns are universal.

Figure 11 shows, by examples, the universal evolution of the densities of log returns across time scales. Each figure in Figure 11 corresponds to a fixed value of the variance and shows the densities of log returns of various markets at time scales that correspond to the fixed value of the variance. For all values of the variances we were able to find time scales from Figure 7 that correspond to the fixed variance. The densities collapse onto universal densities that are independent of the type of market considered (compare to Figure 4 for turbulent data).

## 5 Conclusions

In the present analysis we showed that the marginal densities of log returns for various financial markets collapse after applying a deterministic time change in terms of the variances as a function of time scale  $s$ . This behaviour is completely analogous to what has been earlier demonstrated for isotropic turbulent flows and as such adds a new stylized fact to the empirical similarities between the two fields.

The collapse of densities of log returns and velocity increments for equal variance time scales strongly resembles a Gaussian behaviour for zero mean processes. However in finance and turbulence the densities of log returns/velocity increments are strongly non-Gaussian and the fact that the densities of log returns/velocity increments collapse whenever the corresponding variances are the same is, in our opinion, a far-reaching result.

The time change in terms of the variances that we propose in this paper is deterministic (in contrast to various approaches in finance dealing with stochastic time changes) and directly accessible from data. An important issue is the clarification of whether the SEC relation is kinematic or dynamic, i.e. can we extend the present results to a stochastic relation between the dynamics of the log price process in different markets. An affirmative answer implies that all markets within the SEC share the same stochastic dynamics and are only related by deterministic time changes. To conserve the stationarity of the increments of the involved processes, the time change  $\bar{c}_2^{(i)}(c^{(j)}(s))$  has to be linear in  $s$ . Figure 8 indicates that this is true for financial markets. Work on a clarification of the dynamical content of the SEC relation (12) is currently in progress.

## References

- [1] Antonia, R.A. and Pearson, B.R. (2000): Effect of initial conditions on the mean energy dissipation rate and the scaling exponent. *Phys. Rev. E* **62**, 8086-8090.
- [2] Asmussen, S. and Rosinski, J. (2001): Approximation of small jumps of Lévy processes with a view towards simulation. *J. Appl. Probab.* **38**, 482-493.
- [3] Barndorff-Nielsen, O.E. (1977): Exponentially decreasing distributions for the logarithm of particle size. *Proc. R. Soc. London* **A 353**, 401-419.
- [4] Barndorff-Nielsen, O.E. (1995): Normal inverse Gaussian processes and the modelling of stock returns. Research Report 300, Dept. Theor. Statistics, Aarhus University.
- [5] Barndorff-Nielsen, O.E. (1997): Normal inverse Gaussian distributions and stochastic volatility modelling. *Scand. J. Statist.* **24**, 1-14.

- [6] Barndorff-Nielsen, O.E. (1998a): Probability and statistics: self-decomposability, finance and turbulence. In Accardi, L. and Heyde, C.C. (Eds.): *Probability Towards 2000*. Proceedings of a Symposium held 2-5 October 1995 at Columbia University. New York: Springer-Verlag. Pp. 47-57.
- [7] Barndorff-Nielsen, O.E. (1998b): Processes of normal inverse Gaussian type. *Finance and Stochastics* **2**, 41-68.
- [8] Barndorff-Nielsen, O.E. (1998c): Superposition of Ornstein-Uhlenbeck type processes. *Theory Prob. Its Appl.* **45**, 175-194.
- [9] Barndorff-Nielsen, O.E., Blæsild, P. and Schmiegel, J. (2004): A parsimonious and universal description of turbulent velocity increments. *Eur. Phys. J. B* **41**, 345-363.
- [10] Barndorff-Nielsen, O.E. and Levendorskiĭ, S.Z. (2001): Feller processes of normal inverse Gaussian type. *Quantitative Finance* **1**, 318-331.
- [11] Barndorff-Nielsen, O.E. and Prause, K. (2001): Apparent scaling. *Finance and Stochastics*. **5**, 103-113.
- [12] Barndorff-Nielsen and Schmiegel, J. (2006): Time change and universality in turbulence. Research Report 2006-15, Thiele Centre for Applied Mathematics in Natural Sciences, University of Aarhus. (Submitted.)
- [13] Barndorff-Nielsen, O.E., Schmiegel, J. and Shephard, N. (2006): Quadratic variation and bipower variation under stationary Gaussian processes. (In preparation.)
- [14] Barndorff-Nielsen, O.E. and Shephard, N. (2000): Modelling by Lévy processes for financial econometrics. In O.E. Barndorff-Nielsen, T. Mikosch and S. Resnick (Eds.): *Lévy Processes - Theory and Applications*. Boston: Birkhäuser. (2001). Pp. 283-318.
- [15] Barndorff-Nielsen, O.E. and Shephard, N. (2001): Non-Gaussian OU based models and some of their uses in financial economics (with Discussion). *J. R. Statist. Soc.* **B 63**, 167-241.
- [16] Barndorff-Nielsen, O.E. and Shephard, N. (2002): Integrated OU processes and non-Gaussian OU-based stochastic volatility. *Scand. J. Statist.* **30**, 277-295.
- [17] Barndorff-Nielsen, O.E. and Shephard, N. (2004): Power and bipower variation with stochastic volatility and jumps (with Discussion). *J. Fin. Econometrics***2**, 1-48.
- [18] Barndorff-Nielsen, O.E. and Shephard, N. (2007): *Continuous-Time Approach to Finance. Volatility and Lévy-Based Modelling*. Cambridge University Press. (To appear).
- [19] Chanal, O., Chebaud, B., Castaing, B. and Hébral, B. (2000): Intermittency in a turbulent low temperature gaseous helium jet. *Eur. Phys. J. B* **17**, 309-317.
- [20] Cont, R. and Tankov, P. (2004): *Financial Modelling With Jump Processes*. Chapman & Hall/CRC, London.
- [21] Dacorogna, M., Gencay, R., Müller, U., Olsen, R.B. and Pictet, O.V. (2001): *An Introduction to High-Frequency Finance*. Academic Press, San Diego.



- [22] Dhruva, B. (2000): An experimental study of high Reynolds number turbulence in the atmosphere. PhD Thesis, Yale University.
- [23] Eberlein, E. (2000): Application of generalized hyperbolic Lévy motion to finance. In O.E. Barndorff-Nielsen, T. Mikosch and S. Resnick (Eds.): *Lévy Processes - Theory and Applications*. Boston: Birkhäuser. Pp. 319-336.
- [24] Forsberg, L. (2002): On the Normal Inverse Gaussian distribution in Modelling Volatility in the Financial Markets, *Acta Universitatis Upsaliensis, Studia Statistica Upsaliensia* 5, Uppsala.
- [25] Ghashgaie, S., Breymann, W., Peinke, J., Talkner, P. and Dodge, Y. (1996): Turbulent cascades in foreign exchange markets. *Nature* **381**, 767-770.
- [26] McNeil, A.J., Frey, R. and Embrechts, P. (2005): *Quantitative Risk Management*. Princeton University Press, Princeton.
- [27] Peinke, J., Bottcher, F. and Barth, S (2004): Anomalous statistics in turbulence, financial markets and other complex systems. *Ann. Phys. (Leipzig)* **13**, 450-460.
- [28] Prause, K. (1999): *The Generalized Hyperbolic Model: Estimation, Financial Derivatives and Risk Measures*. Dissertation. Albert-Ludwigs-Universität, Freiburg i. Br.
- [29] Raible, S. (2000): *Lévy Processes in Finance: Theory, Numerics, Empirical Facts*. Dissertation. Albert-Ludwigs-Universität, Freiburg i. Br.
- [30] Rydberg, T.H. (1997): The normal inverse Gaussian Lévy process: simulation and approximation. *Comm. Statist.: Stochastic Models* **13**, 887-910.
- [31] Rydberg, T.H. (1999): Generalized hyperbolic diffusions with applications towards finance. *Math. Finance* **9** , 183-201.
- [32] Sreenivasan, K.R. and Dhruva, B. (1998): Is there scaling in high-Reynolds-number turbulence? *Prog. Theor. Phys. Suppl.* **130**, 103-120.

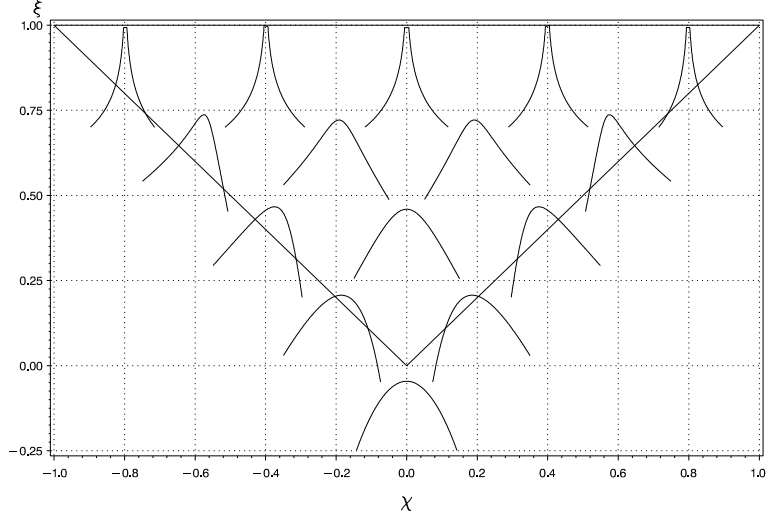


Figure 1: The shape triangle of the NIG distributions with the log density functions of the standardized distributions, i.e. with mean 0 and variance 1, corresponding to the values  $(\chi, \xi) = (\pm 0.8, 0.999), (\pm 0.4, 0.999), (0.0, 0.999), (\pm 0.6, 0.75), (\pm 0.2, 0.75), (\pm 0.4, 0.5), (0.0, 0.5), (\pm 0.2, 0.25)$  and  $(0.0, 0.0)$ . The coordinate system of the log densities is placed at the corresponding value of  $(\chi, \xi)$ .

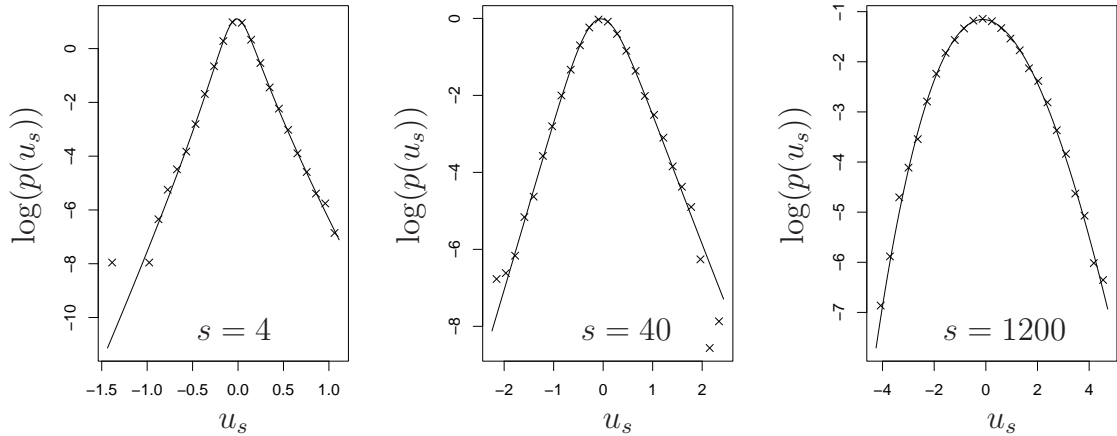


Figure 2: Approximation of the densities  $p(u_s)$  of velocity increments  $u_s$  within the class of NIG distributions (using maximum likelihood estimation of the four parameters  $\alpha, \beta, \delta$  and  $\mu$ ) for data set h929 and time lags  $s = 4, 40, 1200$  (in units of the finest resolution).

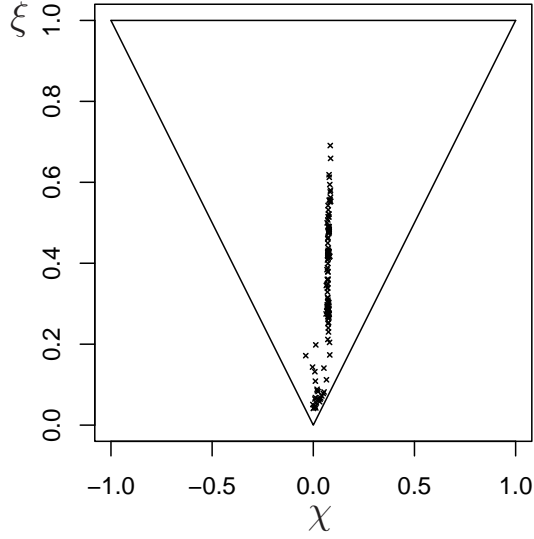


Figure 3: NIG shape triangle for the densities of velocity increments at time scales  $s \in [4, 8000]$  (in units of the finest resolution) for data set h929. Each point corresponds to one time scale  $s$  with the time scales  $s$  increasing from top to bottom.

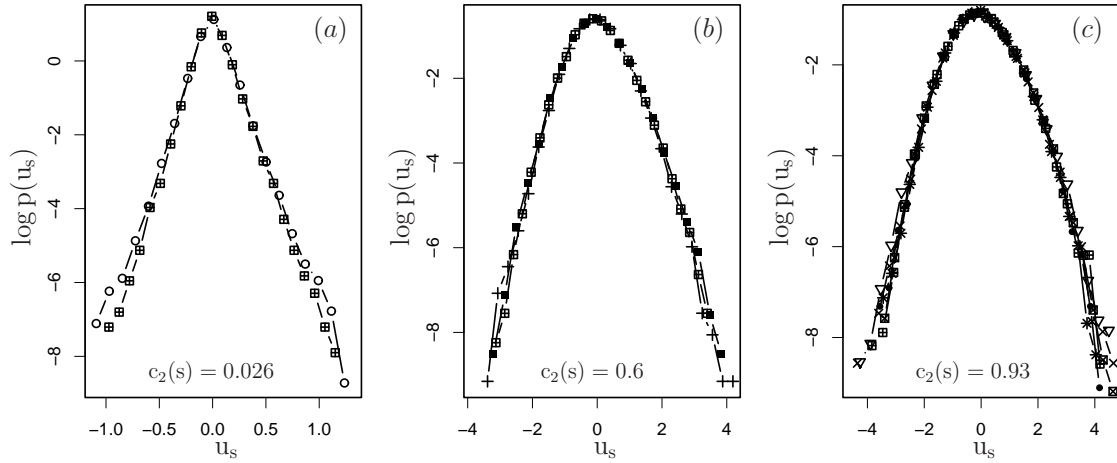


Figure 4: Collapse of the densities  $p(u_s)$  of velocity increments for various fixed values of the variance  $c_2(s)$ . The corresponding values of the time lag  $s$  (in units of the finest resolution of the corresponding data set) and the data sets are (a) ( $s = 116$ , at) ( $\circ$ ), ( $s = 4$ , h352) ( $\boxplus$ ), (b) ( $s = 192$ , h885) ( $\blacksquare$ ), ( $s = 88$ , h352) ( $\boxplus$ ), ( $s = 10$ , w) ( $+$ ) and (c) ( $s = 420$ , h703) ( $\times$ ), ( $s = 440$ , h929) ( $\nabla$ ), ( $s = 180$ , h352) ( $\boxplus$ ), ( $s = 270$ , h283) ( $\bullet$ ), ( $s = 108$ , h124) ( $*$ ), ( $s = 56$ , h85) ( $\boxtimes$ ).

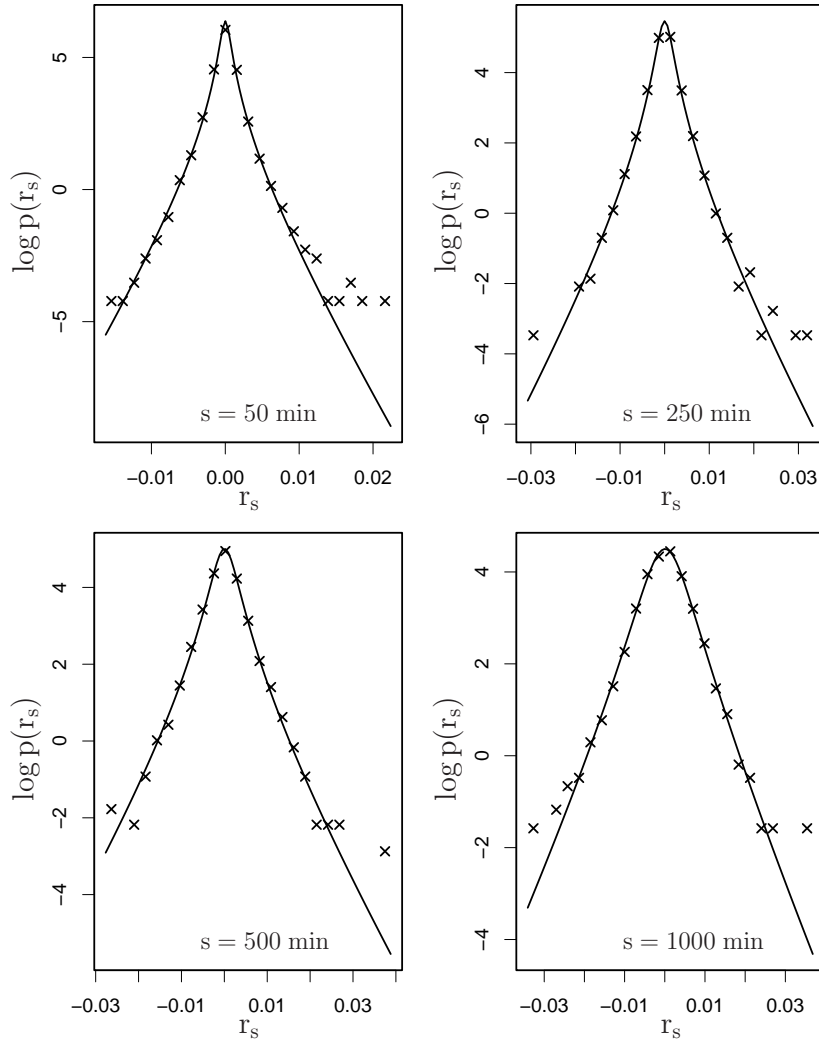


Figure 5: Logarithm of the densities  $p(r_s)$  of log DEM/USD returns at time scales  $s = 50, 250, 500, 1000$  min. The solid lines denote the approximation within the class of NIG distributions using maximum likelihood estimation of the parameters  $\alpha, \beta, \delta$  and  $\mu$ .

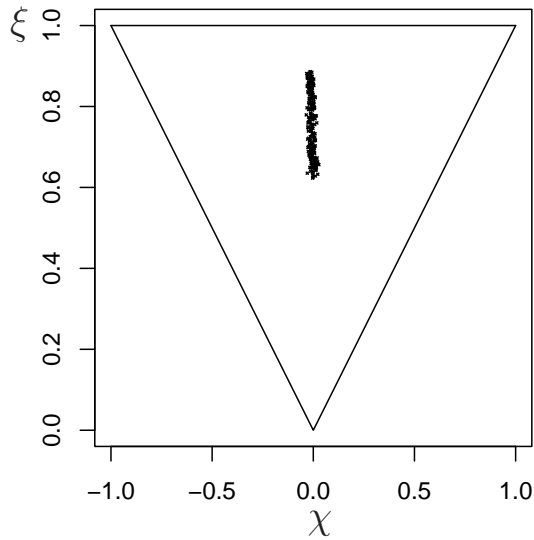


Figure 6: NIG shape triangle for the densities of log DEM/USD returns at time scales  $s \in [1, 290]$  (in units of 5 min). Each point corresponds to one time scale  $s$  with the time scales  $s$  increasing from top to bottom.

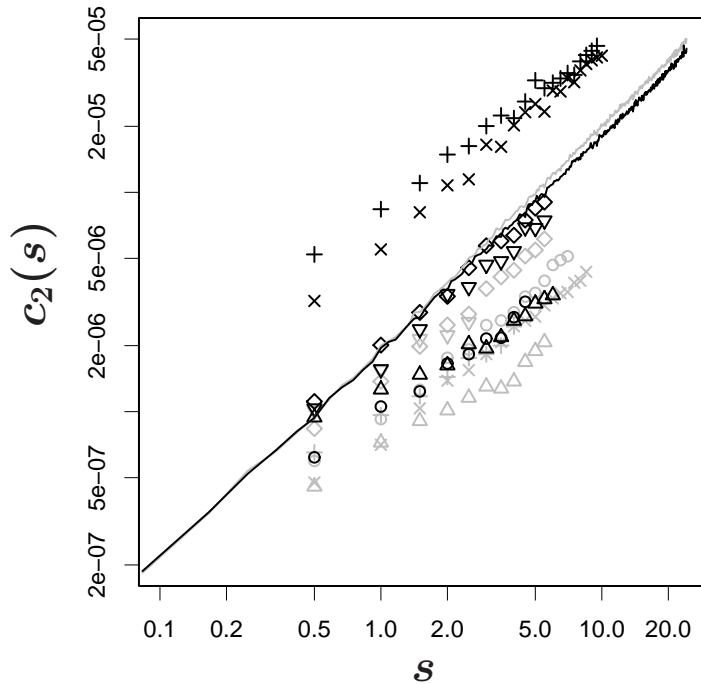


Figure 7: Estimated variances  $c_2(s)$  as a function of the time lag  $s$  (in units of hours) in double logarithmic representation for the data sets AUD/USD ( $\circ$ , grey), DEM/FIM ( $\Delta$ , grey), DEM/ITL ( $+$ , grey), GBP/USD ( $\times$ , grey), USD/CHF ( $\diamond$ , grey), USD/FIM ( $\nabla$ , grey), DEM/USD (grey line), USD/FRF ( $\circ$ , black), USD/ITL ( $\Delta$ , black), XAG/USD ( $+$ , black), XPD/USD ( $\times$ , black), USD/ZAR ( $\diamond$ , black), XPT/USD ( $\nabla$ , black), JPY/USD (black line).

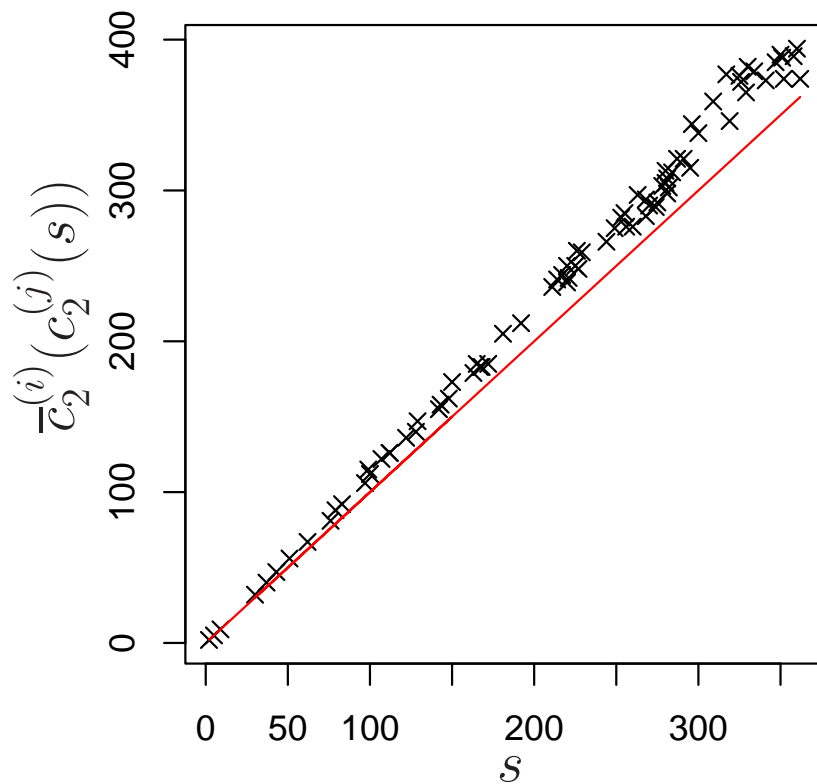


Figure 8: Empirical time change  $\bar{c}_2^{(i)}(c_2^{(j)}(s))$  ( $\times$ ) where  $(i)$  denotes the DEM/USD market and  $(j)$  denotes the JPY/USD market. For comparison, we included the equal-time relation  $\bar{c}_2^{(i)}(c_2^{(j)}(s)) = s$  (solid line).

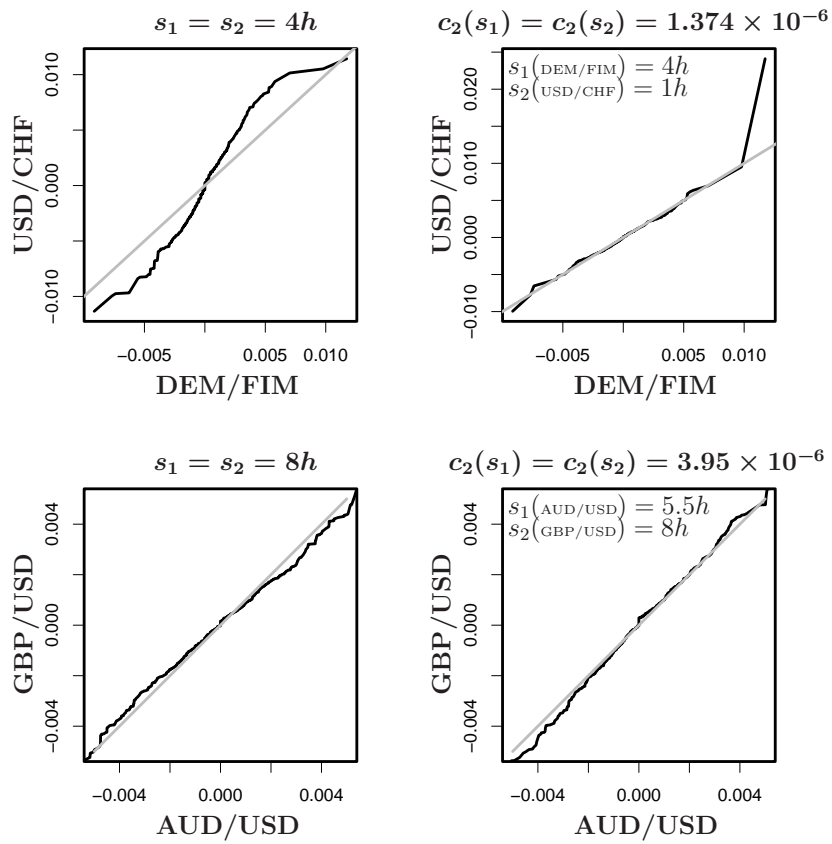


Figure 9: QQ plots of log currency returns at the same time scales  $s_1 = s_2$  and at time scales where the corresponding variances are the same.

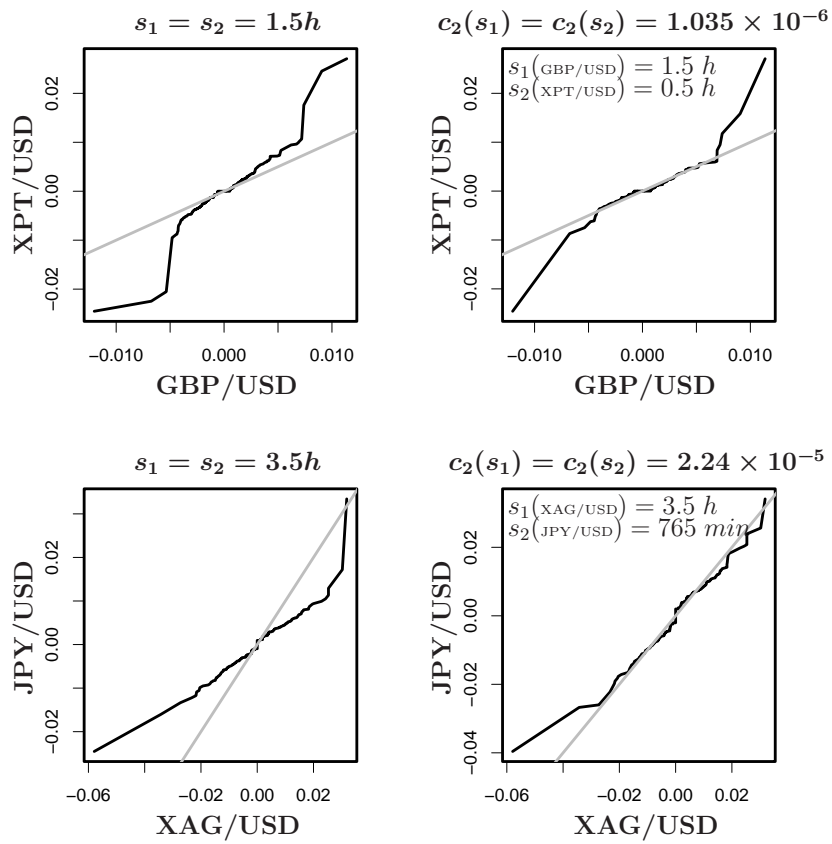


Figure 10: QQ plots of log currency returns and log metal returns at the same time scales  $s_1 = s_2$  and at time scales where the corresponding variances are the same.



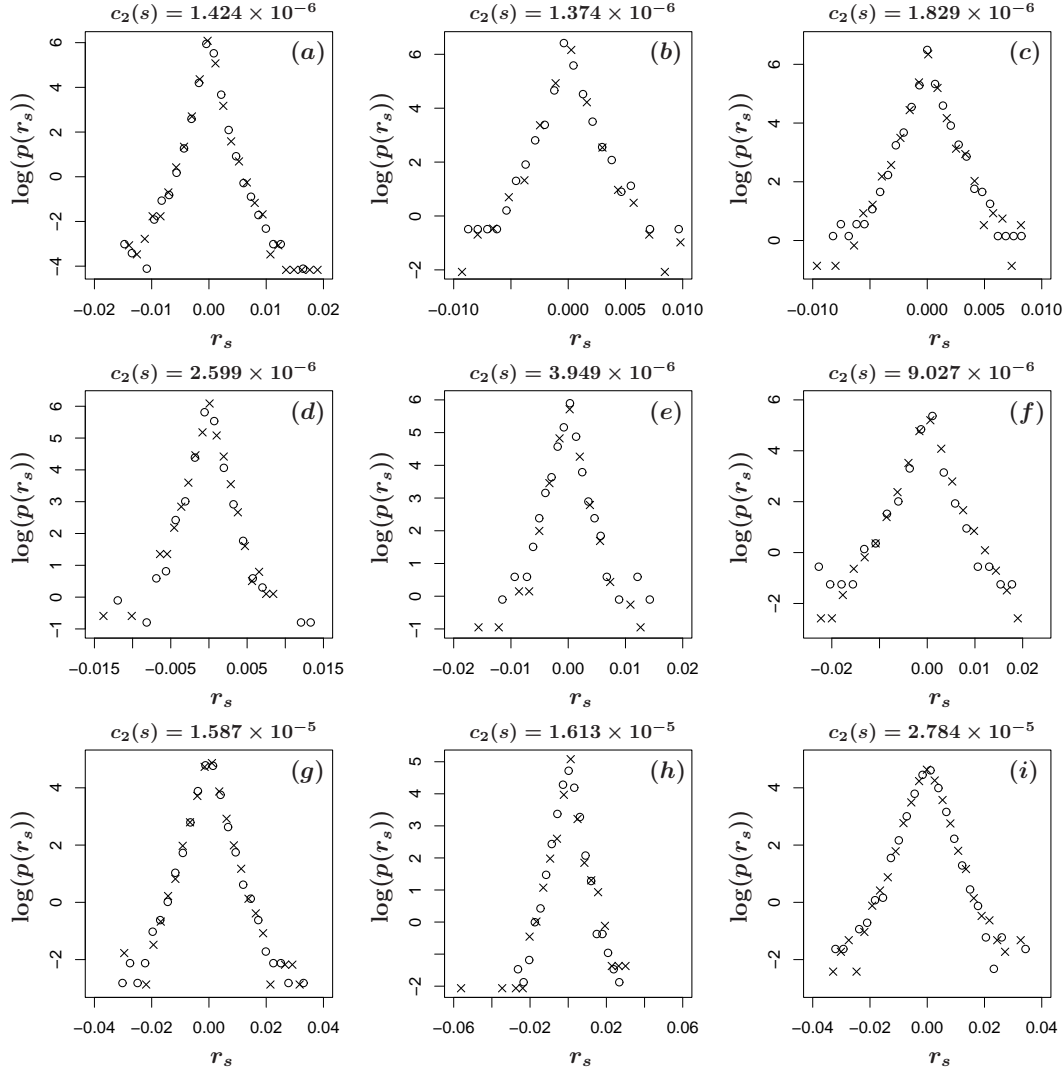


Figure 11: Collapse of the densities  $p(r_s)$  of log returns at time scales  $s$  where the corresponding variances are the same. Time scales  $s$  and data sets are (a) DEM/USD ( $s = 45 \text{ min}$ ,  $\times$ ) and JPY/USD ( $s = 45 \text{ min}$ ,  $\circ$ ), (b) USD/CHF ( $s = 1 \text{ h}$ ,  $\times$ ) and DEM/FIM ( $s = 4 \text{ h}$ ,  $\circ$ ), (c) USD/FRF ( $s = 2.5 \text{ h}$ ,  $\times$ ) and DEM/ITL ( $s = 3 \text{ h}$ ,  $\circ$ ), (d) USD/ITL ( $s = 4 \text{ h}$ ,  $\times$ ) and GBP/USD ( $s = 4.5 \text{ h}$ ,  $\circ$ ), (e) AUD/USD ( $s = 5.5 \text{ h}$ ,  $\times$ ) and GBP/USD ( $s = 8 \text{ h}$ ,  $\circ$ ), (f) DEM/USD ( $s = 275 \text{ min}$ ,  $\times$ ) and USD/ZAR ( $s = 5.5 \text{ h}$ ,  $\circ$ ), (g) DEM/USD ( $s = 8 \text{ h}$ ,  $\times$ ) and JPY/USD ( $s = 525 \text{ min}$ ,  $\circ$ ), (h) XAG/USD ( $s = 3.5 \text{ h}$ ,  $\times$ ) and JPY/USD ( $s = 765 \text{ min}$ ,  $\circ$ ), (i) DEM/USD ( $s = 825 \text{ min}$ ,  $\times$ ) and JPY/USD ( $s = 925 \text{ min}$ ,  $\circ$ ),